Reproductive Toxicology 53 (2015) 141–151

Contents lists available at ScienceDirect

Reproductive Toxicology

journal homepage: www.elsevier.com/locate/reprotox

Effects of mono(2-ethylhexyl)phthalate on cytoplasmic maturation of oocytes – The bovine model

D. Kalo, Z. Roth*

Department of Animal Sciences, Robert H. Smith Faculty of Agriculture, Food and Environment, and Center of Excellence in Agriculture and Environmental Health, the Hebrew University, Rehovot 76100, Israel

ARTICLE INFO

Article history:
Received 20 November 2014
Received in revised form 9 March 2015
Accepted 3 April 2015
Available online 18 April 2015

Keywords:
Phthalate
Oocyte
Cytoplasmic maturation
Bovine

ABSTRACT

Phthalates are known reproductive toxicants, but their intracellular disruptive effects on oocyte maturation competence are less known. We studied the potential risk associated with acute exposure of oocytes to mono(2-ethylhexyl)phthalate (MEHP). First, bovine oocytes were matured in vitro with or without 50 μM MEHP and examined for mitochondrial features associated with DNA fragmentation. MEHP increased reactive oxygen species levels and reduced the proportion of highly polarized mitochondria along with alterations in genes associated with mitochondrial oxidative phosphorylation (*CYC1*, *MT-CO1* and *ATP5B*). In a second set of experiments, we associated the effects of MEHP on meiotic progression with those on cytoplasmic maturation. MEHP impaired reorganization of cytoplasmic organelles in matured oocytes reflected by reductions in category I mitochondria, type III cortical granules and class I endoplasmic reticulum. These alterations are associated with the previously reported reduced developmental competence of MEHP-treated bovine oocytes, and reveal the risk associated with acute exposure.

1. Introduction

Phthalates are used as plasticizers in plastic and PVC products [1], and are ubiquitous in the environment [2]. They are known as endocrine-disruptors (EDs) that deleteriously affect developmental and reproductive function in both males and females [2–5]. As EDs, they can interfere with the endocrine system; however, whether their effects on oocytes are adverse or adaptive (i.e., non-adverse) is less well understood [6].

Humans and animals can potentially be exposed to DEHP via contaminated food, the air indoors or household items [2]. However, exposure to relatively high doses of DEHP is mostly due to intensive use of PVC-based devices for medical procedures [2], such as blood transfusions and hemodialysis in infants [7]. DEHP concentrations in blood bags range from 1.8 to 83.2 μg/ml [8]. In addition, MEHP levels in red blood cells packed for storage have been found to increase 20-fold – from 3.7 μM on day 1 to 74 μM on day 42 [9] – the latter level similar to that used in the current study. The most abundantly used phthalates, di(2-ethylhexyl)phthalate (DEHP) and its primary metabolite mono(2-ethylhexyl)phthalate (MEHP), have been detected in human serum (6.74 ng/ml), seminal plasma (0.45 ng/ml) [10], cord blood serum (0.52 μg/ml) [11], urine (4.49–9.18 ng/ml) [10–13], and peritoneal (0.37 μg/m) [14] and amniotic fluids (2.8 ng/ml) [15].

In vitro studies in mouse have shown that exposure to a wide range of DEHP doses (10 and 100 μM) has a negative impact on primordial follicle assembly [16], and on follicular growth and estradiol production in antral follicles (100 μg/ml) [17]. Other studies have shown a deleterious effect on meiotic progression in ovines (0.12 μM) [18], and on fertilization ability and embryonic development in bovines (50 μM) [19] and in mice (1 μg/ml) [20]. Lenie and Smitz [21] showed that exposure to 10–200 μM MEHP has only a minor effect on steroidogenesis in mouse follicles, with no effect on oocyte meiotic progression. In contrast, 45–180 μM MEHP induced an oxidative response in human placental cells [22], and inhibited follicular development in rats at doses higher than 0.036 nM [23]. MEHP at 10 μg/ml reduced CCND2, CDK4 and aromatase mRNA expression in the mouse antral follicle [17], and at 250 and 500 μM, it altered mouse oocyte viability in association with SOD1 and ND1 mRNA expression [24].

The oocyte reaches competence through the lengthy processes of folliculogenesis and oocyte growth, which involve both nuclear and cytoplasmic maturation. Growth of mammalian oocytes is arrested in the ovarian follicle at the diplotene stage of the first meiotic prophase, termed the germinal vesicle (GV) stage. As maturation progresses, the oocyte resumes meiosis and progresses to

* Corresponding author. Tel.: +972 8 9489103; fax: +972 8 9465763.
E-mail address: roth@agri.huji.ac.il (Z. Roth).

http://dx.doi.org/10.1016/j.reprotox.2015.04.007
0890-6238/

form the second metaphase (MII) plate accompanied by the first polar body extrusion [25]. In bovines, concentrations of MEHP ranging between 10 and 250 μM have been shown to impair oocyte nuclear maturation in a dose-responsive manner. According to Beker van Woudenberg et al. [26], MEHP at a concentration 217 μM is potent enough to impair oocyte meiotic progression. In our previous study, we reported that exposure of cumulus oocyte complexes (COCs) to 50 μM MEHP for 22 h impairs nuclear maturation, whereas 25 or 100 μM only increased the number of TUNEL-positive oocytes [19]. On the other hand, Anas et al. [27] reported that exposure of bovine COCs to 25 μM MEHP impairs nuclear maturation.

Less is known about the effects of phthalates on oocyte cytoplasmic maturation. Studies have shown that cytoplasmic maturation consists of multiple events that are essential for fertilization and early embryonic development [29,30]. These include reorganization of the cytoskeletal filaments and redistribution of cytoplasmic organelles, including the mitochondria, cortical granules (CGs) and endoplasmic reticulum (ER), through the actions of cytoskeletal microfilaments and microtubules [31,32]. In bovines, the mitochondria relocate from the restricted peripheral region at the GV stage into a diffuse pattern throughout the cytoplasm center at the MII stage [33,34]. Studies in rodents [35–37], humans [38] and bovines [39] have shown a similar pattern of ER relocation, from a fine network spread throughout the interior cytoplasm at the GV stage to an accumulation of bright cortical clusters in the cortex at the MII stage. Studies in bovines [40,41], and mice [42] have shown that CG distribution changes from a dispersed pattern throughout the cytoplasm at the GV stage to an even dispersion in a thin layer lining the oolemma at the MII stage.

In our previous study, in vitro maturation (IVM) with 50 μM MEHP impaired the developmental competence of bovine oocytes [19], reflected by a reduced proportion of oocytes that showed nuclear maturation, reached the MII-stage, were fertilized, underwent first cleavages and developed to the blastocyst stage [19]. Given that oocyte maturation is a prerequisite for successful fertilization and is highly correlated with embryonic development [28,43], the aim of the current study was to examine the potential risk posed by phthalate exposure to oocyte cytoplasmic maturation. We utilized bovine oocytes and an IVM procedure as research tools to examine the effects of relatively high dose (50 μM MEHP), similar to the level found in PVC-based red blood cell bags [9], on cytoplasmic organelle reorganization and function, including mitochondrial distribution and function, CG reorganization and ER relocation.

2. Materials and methods

All chemicals were purchased from Sigma (Rehovot, Israel) unless otherwise indicated.

2.1. Oocyte collection and IVM

Bovine ovaries were obtained from a local abattoir and transported to the laboratory within 60–90 min in physiological saline solution (0.9%, w/v NaCl at 38.5 °C with 50 μg/ml penicillin–streptomycin). COCs were aspirated from 3- to 8-mm follicles with an 18-gauge needle attached to a 10-ml syringe. They were collected into Hepes–Tyrode's lactate (TL) prepared in our laboratory [44], supplemented with 0.3% (w/v) bovine serum albumin (BSA), 0.2 mM sodium pyruvate and 0.75 mg/ml gentamicin at 38.5 °C (Hepes–TALP). At the end of the collection, COCs with at least three layers of cumulus surrounding a homogeneous cytoplasm were selected for IVM.

Selected COCs were washed three times in Hepes–TALP and groups of 10 were transferred into 50-μl droplets of oocyte maturation medium (OMM) made up of TCM-199 and Earle's salts supplemented with 10% (v/v) heat-inactivated fetal calf serum (Promega, Madison, WI, USA), 0.2 mM sodium pyruvate, 50 μg/μl gentamicin, 2.2 g/l sodium bicarbonate, 2 μg/ml 17-β estradiol and 1.32 μg/ml follicle-stimulating hormone (Folltropin-V; Bioniche Animal Health, Belleville, Ontario, Canada). The COC-containing droplets were overlaid with mineral oil and incubated in humidified air with 5% CO_2 for 22 h at 38.5 °C.

2.2. Classification of oocyte meiotic status

The meiotic status of each oocyte was determined using the cell-permeant DNA dye 4′,6-diamidino-2-phenylindole dihydrochloride (DAPI). Oocytes were fixed in 2% (v/v) paraformaldehyde (Electron Microscopy Sciences, Hatfield, PA, USA) in Dulbecco's phosphate buffered saline (PBS; Promega) for 15 min at room temperature and stored in PBS supplemented with 1 mg/ml polyvinylpyrrolidone (PBS–PVP) at 4 °C. Before staining, oocytes were washed three times in PBS–PVP and labeled with 10 μg/ml DAPI in PBS–PVP for 15 min at room temperature. Stained oocytes were classified into germinal vesicle (GV), germinal vesicle breakdown (GVBD), metaphase I (MI), anaphase I (AI) and telophase I (TI) stages, or MII stage with an extruded first polar body (PB). Oocytes at the GV, GVBD, MI, AI and TI stages and those with abnormal chromosomal organization were classified as immature oocytes; MII-stage oocytes were classified as mature.

2.3. Assessment of mitochondrial features

2.3.1. Measurements of reactive oxygen species (ROS)

Oocytes were stained with 2′,7′-dichlorodihydrofluorescein diacetate (H_2DCFDA) as previously described for bovine oocytes [45–47] with some modifications. H_2DCFDA is a cell-permeant fluorogenic reagent. In the cell, it is deacetylated to H_2DCF, which can then be oxidized by ROS to the highly fluorescent compound 2′,7′-dichlorofluorescein (DCF), thus reflecting ROS levels. Briefly, oocytes were incubated in 100 μM H_2DCFDA at 38.5 °C and 5% CO_2 for 30 min, then washed in Hepes–TALP and immediately examined under an inverted fluorescence microscope using Nis Elements software (Nikon, Tokyo, Japan). Intracellular fluorescence of DCF was measured (excitation at 450–490 nm and emission at 515–565 nm) in oocytes (in groups of 5) over 30 s at three time points: 0–10 s, 11–20 s and 21–30 s. The wavelengths and exposure times were held constant for all oocytes during the time of measurement. The intensity of the fluorescent signal was quantified using ImageJ software version 1.4 (National Institutes of Health, Bethesda, MD, USA) by measuring brightness for each oocyte. A circle was drawn around each measured oocyte and the fluorescence intensity was recorded. Measurement of a blank circled area was recorded for normalization.

2.3.2. Mitochondrial membrane polarity

Mitochondrial membrane polarity was evaluated with the Mitocapture mitochondrial apoptosis detection fluorometric kit (Biovision, Milpitas, CA, USA) as previously performed in our laboratory [48]. Briefly, live denuded oocytes were incubated in Mitocapture diluted in prewarmed incubation buffer (1:10, v/v) at 38.5 °C for 20 min. Oocytes were then examined under an inverted fluorescence microscope using Nis Elements software. The kit's cationic dye exhibits potential-dependent accumulation in mitochondria, indicated by a fluorescence-emission shift from green to red (low to highly polarized potential). Each individual oocyte was visualized under the inverted fluorescence microscope using the FITC channel for green monomers (excitation at 450–490 nm and emission at 515–565 nm) and the PI channel for red aggregates (excitation at 488 nm and emission at 590 nm). The

Table 1
Primers used for qPCR.

Gene	Primer	Accession number	Sequence (5′→3′)	Size (bp)
MT-ND2	Forward Reverse	NM_174565	CATGCTCCGAAACTCTGACA GCATTTACACAGGCCCCTAA	129
SDHB	Forward Reverse	NM_1040483	GTCCTATGGTGCTGGATGCT GTTGATGTTCATGGCACAGG	113
CYC1	Forward Reverse	NM_1038090	CCAGGTAGCCAAGGATGTGT CTTTCGGCTCTTGAGGACTG	163
MT-CO1	Forward Reverse	JX567086	AACAGGCTGAACCGTGTACC TACGAACAGAGGGGTTTGGT	118
ATP5B	Forward Reverse	NM_175796	TGCTTTATTGGGCAGAATCC GATCCGTCAAGTCATCAGCA	152
YWHAZ	Forward Reverse	NM_174814	GCATCCCACAGACTATTTCC GCAAAGACAATGACAGACCA	124

intensity of the fluorescent signal was quantified using ImageJ software by measuring brightness for each oocyte and the red/green ratio was calculated. The cutoff between high- and low-polarized mitochondria was based on the calculated red/green ratio: a value higher than 1 was taken to indicate relatively high-polarized mitochondria and a value lower than 1, relatively low-polarized mitochondria.

2.3.3. Evaluation of transcript abundance by real-time quantitative (q) PCR

For each experimental group, 20 oocytes per sample from 6 replicates were collected at the end of 22 h maturation and stored at −80 °C until mRNA extraction. Poly(A) RNA was isolated using Dynabeads mRNA DIRECT Kit according to the manufacturer's instructions (Life Technologies) as previously performed in our lab and described by [44,48]. Real-time qPCR was carried out with primers for *MT-ND2*, *SDHB*, *MT-CO1*, *CYC1* and *ATP5B*, using *YWHAZ* as the reference gene. The selected genes encode subunits of the five complexes (I–V) associated with mitochondrial oxidative phosphorylation (OXPHOS). *MT-ND2* and *MT-CO1* are mitochondrial genes encoding subunits of complex I and complex III, respectively; *SDHB*, *CYC1* and *ATP5B* are nuclear genes encoding subunits of complexes II, IV and V, respectively. Specific pairs of primers were designed using Primer 3.0 software (Table 1), derived from bovine sequences found in Genbank and confirmed using BLAST analysis against the genomic data base. Real-time PCR was conducted on an Mx3000p cycler (Stratagene, La Jolla, CA, USA) using DyNAmoColorFlash SYBR® Green qPCR Kit (Finnzymes, Espoo, Finland) in a final volume of 20 μl containing ultra-pure water (Biological Industries), 500 nM of each primer, and 3 μl diluted cDNA. The reaction efficiency ranged between 90 and 110% with $R^2 > 0.995$. The amplification program included preincubation at 95 °C for 7 min to activate taq polymerase, followed by 40 amplification cycles of denaturation at 95 °C for 10 s and annealing–elongation at 60 °C for 15 s. All samples were run in duplicate in 96-well plates. A melting-curve analysis was performed at the end of the amplification to confirm single-gene specificity. Fluorescence was recorded to determine the threshold cycle during the log-linear phase of the reaction at which fluorescence rises above background. Gene expression was quantified and analyzed by MxPRO QPCR software for Mx3000p and Mx3005p QPCR version 3 and the ΔΔCt method was used to calculate the relative expression abundance of each transcript.

2.4. Detection of DNA fragmentation

Oocytes were evaluated for DNA fragmentation by terminal deoxynucleotidyltransferase dUTP nick end labeling (TUNEL) assay (Roche, Basel, Switzerland) as previously performed in our laboratory [49]. Briefly, oocytes were fixed in 2% paraformaldehyde in PBS for 15 min at room temperature and stored in PBS–PVP at 4 °C. Oocytes were washed three times in PBS–PVP and placed in permeabilization solution containing PBS with 1 mg/ml PVP, 0.3% (v/v) Triton X-100 and 0.1% (w/v) sodium citrate for 20 min at room temperature in a humidified box followed by TUNEL assay. Finally, samples were counterstained with 10 μg/ml DAPI in PBS–PVP for 15 min at room temperature and washed three times in PBS–PVP. TUNEL labeling was examined under an inverted fluorescence microscope using Nis Elements software. TUNEL-positive oocytes exhibited green labeling of the MII plate or dual labeling of the MII plate and PB, while green labeling of the PB alone was not included. Positive and negative controls were performed according to the manufacturer's instructions.

2.5. Cytoplasmic organelle labeling

2.5.1. Mitochondrial distribution

Mitochondrial distribution, regardless of membrane potential, was determined by staining with MitoTracker green dye (Life Technologies, Invitrogen, Carlsbad, CA, USA) as performed previously in our laboratory [48]. Live denuded oocytes were incubated in 200 nM MitoTracker green dye in prewarmed Hepes-TALP at 38.5 °C for 30 min, counterstained with 1 μg/ml Hoechst 33342, and examined under an inverted fluorescence microscope using Nis Elements Software. Oocytes were classified into three different mitochondrial-distribution categories associated with cytoplasmic maturation as previously described by [34] for bovine oocytes, with minor modifications. Similar mitochondrial distribution patterns with different classifications have been reported for other species [50–53]: category I – oocytes with mitochondria spread diffusely throughout the oocyte cytoplasm, with or without mitochondrial localization around the perinuclear region, representing cytoplasmically mature oocytes; category II – aggregation of a small number of mitochondrial clumps restricted to the oocyte cortex, with or without mitochondrial localization around the perinuclear region, representing cytoplasmically immature oocytes; category III – intensive green fluorescent staining of mitochondria, representing degenerated oocytes.

2.5.2. CG distribution

Oocytes were subjected to CG-distribution analysis as previously performed in our laboratory [54]. Briefly, oocytes were placed in permeabilization solution containing PBS–PVP supplemented with 0.1% Triton X-100 for 5 min at 39 °C in the oven. Then oocytes were fixed in 2% paraformaldehyde and stored in PBS–PVP at 4 °C. Oocytes were washed three times in PBS–PVP and placed

in blocking solution [PBS supplemented with 1 mg/ml 0.1% Triton X-100, 2%, v/v normal goat serum, 0.1 M glycine, 1%, w/v powdered skim milk (Becton, Dickinson and Company, Sparks, MD, USA) and 0.5%, w/v BSA at pH 7.4] for 1 h at 39 °C in the oven. After three washes in PBS–PVP, oocytes were stained with 100 μg/ml fluorescein isothiocyanate-conjugated Arachis hypogaea agglutinin (FITC-PNA) in PBS–PVP for 30 min at 39 °C in the oven. All oocytes were counterstained with 10 μg/ml DAPI and CG pattern was classified under an inverted fluorescence microscope using Nis Elements software according to the distributional pattern defined by [41]: type I – CG aggregates distributed throughout the cytoplasm, representing cytoplasmically immature oocytes; type II – CGs localized mainly in the cortical cytoplasm and distributed as individual particles as well as small aggregates, representing partially cytoplasmically mature oocytes; type III – CGs more or less evenly dispersed in the cortical cytoplasm lining the oolemma, representing fully cytoplasmically mature oocytes.

2.5.3. ER distribution

ER distribution was evaluated by ER-ID red assay kit (Enzo Life Sciences Inc., Sciences Inc., Lausanne, Switzerland) which contains an ER-selective cell-permeable dye. Staining was performed according to the manufacturer's instructions. Briefly, oocytes were incubated in 1 μl ER dye and 2 μl Hoechst 33342 in 1 ml prewarmed ER buffer at 38.5 °C, 5% CO_2 for 30 min. Oocytes were then washed three times in Hepes–TALP and examined under an inverted fluorescence microscope using Nis Elements software. ER distribution was evaluated according to the classification previously described for mammals [35–39], with some minor modifications: class I – cytoplasmically mature oocytes, characterized by bright fluorescence and distribution of the ER near the oocyte cortex and membrane including, or not, the first PB region; class II – cytoplasmically immature oocytes, characterized by ER dispersed throughout the oocyte cytoplasm with only a few, if any, clusters in the cortex; class III – degenerated oocytes, characterized by an intense red fluorescence signal dispersed throughout the entire oocyte cytoplasm with large clusters.

2.6. Experimental design

The study included two sets of experiments which were both performed during the winter season to avoid any summer effect on the oocytes. For all analyses, COCs were randomly assigned to a control group cultured in standard OMM, and a treated group cultured in OMM with 50 μM MEHP (Wako Chemicals, Neuss, Germany) dissolved in dimethyl sulfoxide (DMSO) at a maximum concentration of 0.07% (v/v). At the end of 22 h culture, oocytes were denuded of cumulus cells by gentle vortexing in Hepes–TALP containing 1000 IU/ml hyaluronidase, and washed three times in Hepes–TALP. The concentration of MEHP used was based on our preliminary dose-response study (25, 50 and 100 μM), in which a dose of 50 μM was found to reduce the proportion of oocytes that undergo nuclear maturation, fertilization and development to the blastocyst stage, but did not have a lethal effect on the entire cohort of examined oocytes [19].

The effect DMSO on oocyte meiotic status ($n = 30$ oocyte/group; 7 replicates), and ER ($n = 35$ oocyte/group; 5 replicates) and CG ($n = 23$ oocyte/group; 3 replicates) distribution was also examined on a subset of oocytes. It was found that 0.07% (v/v) DMSO did not affect the proportion of MII-stage oocytes (63% vs. 63.4% for control and DMSO-treated oocytes, respectively; $P < 0.9$). In addition, DMSO did not affect the patterns of either ER or CG distribution into different classes/types ($P < 0.68$ and $P < 0.75$, respectively), reflected by a similar proportion of oocytes with class I ER (60.3% vs. 64.7% for control and DMSO-treated, respectively) and type III CG (43.7% vs. 43.3% for control and DMSO-treated, respectively).

The first set of experiments (Experiment 1) was performed to examine the effects of MEHP on mitochondrial features that might be associated with DNA fragmentation: live denuded oocytes were stained with Mitocapture to assess mitochondrial membrane polarity ($n = 45$ oocyte/group; 3 replicates), or with H_2DCFDA to assess ROS production ($n = 40$ oocyte/group; 3 replicates). Another subgroup of oocytes ($n = 20$ oocyte/group; 6 replicates) was subjected to mRNA extraction to determine transcript abundance by qPCR. Finally, another subgroup of oocytes ($n = 29$ oocyte/group; 3 replicates) was stained for TUNEL assay and counterstained with DAPI to evaluate DNA fragmentation.

The second set of experiments (Experiment 2) was performed to associate the effects of MEHP on nuclear maturation with those on cytoplasmic maturation (i.e., organelle distribution). For control and MEHP-treated groups, live oocytes ($n = 35$ oocyte/group; 3 replicates) were stained with Hoechst 33342 to determine their meiotic status and counterstained with MitoTracker green to determine mitochondrial distribution. Another subgroup of oocytes ($n = 43$ oocyte/group; 3 replicates) was fixed and stained with DAPI to determine meiotic status and counterstained with FITC-PNA to observe CG distribution. A third subgroup of oocytes ($n = 35$ oocyte/group; 3 replicates) was stained with ER-ID red to determine ER distribution and counterstained with Hoechst 33342 to determine oocyte meiotic status.

2.7. Statistical analyses

Data were analyzed using JMP-7 software (SAS Institute Inc., 2004, Cary, NC, USA). Overall comparison of treatments for incidence data was performed by chi-square followed by Pearson test. Variables were: nuclear meiotic status, TUNEL labeling, mitochondrial categories, CG types and ER classes. Pairs of treatments were also compared by chi-square followed by Fisher's exact test. ROS content, mitochondrial membrane potential and relative transcript levels were analyzed by one-way ANOVA followed by Student's t test. Before analysis, data were arcsine-transformed. Data are presented as means ± SEM. For all analyses, $P < 0.05$ was considered significant, and P-values between 0.05 and 0.1 were also reported as trends that might be real and worthy of note.

3. Results

3.1. Experiment 1

3.1.1. Effect of MEHP on mitochondrial features associated with DNA fragmentation

Examination of DCF fluorescence intensity from 0 to 30 s postmaturation revealed a linear increase throughout the time interval in both control ($y = 16.06 + 2.86 \times x$; $r = 0.998$) and MEHP-treated ($y = 17.39 + 3.34 \times x$; $r = 0.996$) groups. Nevertheless, MEHP increased the level of ROS, as reflected by stronger DCF fluorescence intensity in the first ($P < 0.07$), second and third ($P < 0.05$; Fig. 1A, A′, A″) measurements.

The proportion of oocytes with highly polarized mitochondrial membranes was lower in the MEHP-treated group relative to the controls (51.11% vs. 75.76%; $P < 0.0001$), as expressed by a lower (<1) red/green fluorescence ratio (Fig. 1B, B′, B″; $P < 0.05$).

MEHP altered the transcript abundance of mitochondrion-associated genes, reflected by lower mRNA levels ($P < 0.05$) for *CYC1* and *MT-CO1* and a higher level ($P < 0.05$) for *ATP5B* in MEHP-treated oocytes relative to the control group (Fig. 1C).

MEHP increased the proportion of TUNEL-positive oocytes relative to the control group (Fig. 2A; $P < 0.007$). Taking into account the meiotic status of the oocytes, further analysis revealed that the proportion of TUNEL-positive oocytes within the group of immature

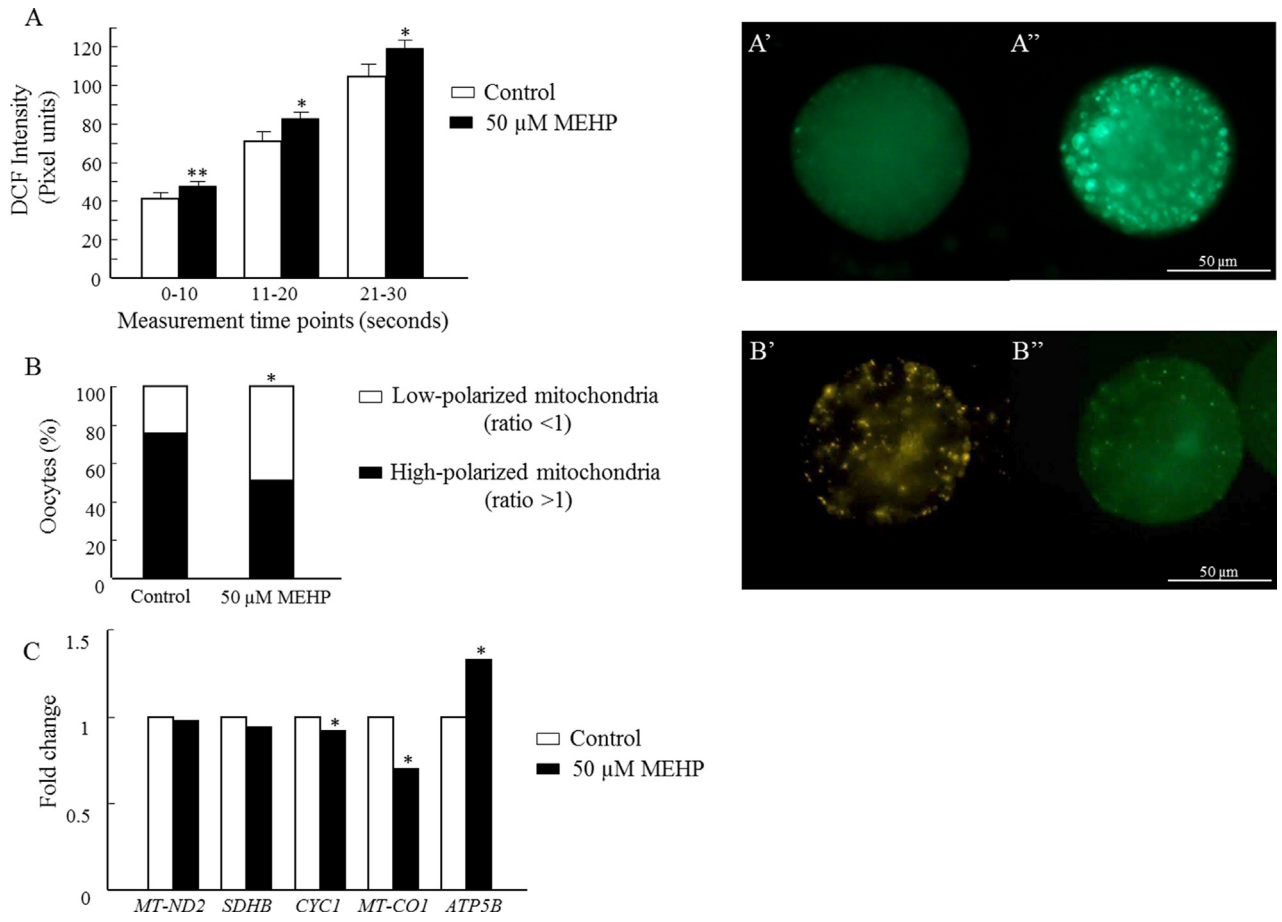

Fig. 1. Effect of MEHP on mitochondrial features. Oocytes were cultured for 22 h in OMM without (control) or with 50 µM MEHP. (A) DCF fluorescence intensity, measured between 0–10, 11–20 and 21–30 s post-oocyte maturation. Data are presented as means ± SEM; $^{*}P<0.05$ and $^{**}P<0.07$ within each time point. Presented are representative images of live oocytes stained with H_2DCFDA expressing low (A′) or high (A″) DCF fluorescence intensity; (B) proportion of oocytes with high- and low-polarized mitochondrial membrane in control and MEHP-treated groups. Representative images of live oocytes stained with Mitocapture mitochondrial apoptosis kit expressing high (B′, red) and low (B″, green) polarized mitochondria. The cutoff between high- and low-polarized mitochondria was based on the calculated red/green ratio, whereby a value higher than 1 was considered indicative of relatively high-polarized mitochondria and a value lower than 1 indicated relatively low-polarized mitochondria. Data are presented as the proportion of oocytes in each polarized mitochondrial state, calculated out of the total number of oocytes in each group. $^{*}P<0.05$; (C) effect of MEHP on transcript abundance of specific electron-transport-chain-associated transcripts. Presented are transcript levels in oocytes collected at the end of 22 h maturation. The ΔΔCT method was used to calculate the real-time RT-PCR fold change using *YWHAZ* mRNA for normalization, and all changes in expression are relative to the control, which was converted to 1. Statistical analyses were performed on the normalized expression (i.e., the target mRNA/internal control mRNA ratio) between groups; $^{*}P<0.05$ within each examined gene. (For interpretation of the references to color in this figure legend, the reader is referred to the web version of the article.)

oocytes did not differ between control and MEHP-treated groups (Fig. 2B; $P=0.82$). On the other hand, the proportion of TUNEL-positive oocytes within the group of mature oocytes was higher in the MEHP-treated vs. control group (Fig. 2C and D; $P<0.0008$).

In light of these findings, another set of experiments (Experiment 2) was therefore performed to examine the association between nuclear status and MEHP-induced cytoplasmic alterations.

3.2. Experiment 2

3.2.1. MEHP effect on cytoplasmic organelle reorganization

Performing the analysis out of total oocytes revealed that MEHP alters the pattern of oocyte distribution within different mitochondrial categories ($P<0.0002$). In particular, MEHP reduced the proportion of oocytes with category I mitochondria relative to the control (47.92% vs. 75.53%, respectively; $P<0.0001$). MEHP also impaired the pattern of oocyte distribution within the different ER classes ($P<0.0001$), expressed mainly by a reduction in the proportion of oocytes with class I ER relative to the control (7.84% vs. 68.83%, respectively; $P<0.0001$). Finally, MEHP altered the pattern of oocyte distribution into different CG types ($P<0.005$), expressed by a reduction in the proportion of oocytes with type III CG relative to the control (38.1% vs. 51.61%; respectively; $P<0.04$).

3.2.2. Association between MEHP-induced alterations in cytoplasmic maturation and meiotic progression

The distribution into different meiotic stages at the end of maturation differed between the control and MEHP-treated groups, with prominent differences in the proportion of TI- and MII-stage oocytes ($P<0.0001$; Table 2). Taken together, the proportion of oocytes defined as mature was higher in the control group than in MEHP-treated group (68.14% vs. 36.36%; $P<0.0001$). In the control group, the reorganization pattern of mitochondria and ER, but not that of CGs, differed between mature and immature oocytes, with a high correlation between mitochondrial category I and ER class I and MII stage (Fig. 3A and D; C and F; $P<0.05$), reflecting the organelles' reorganization dynamics through oocyte maturation. On the other hand, in the MEHP-treated group, the pattern of organelle distribution did not differ between mature and immature oocytes, suggesting a negative effect of MEHP on cytoplasmic maturation (Fig. 3). It should be noted that the proportion of oocytes with

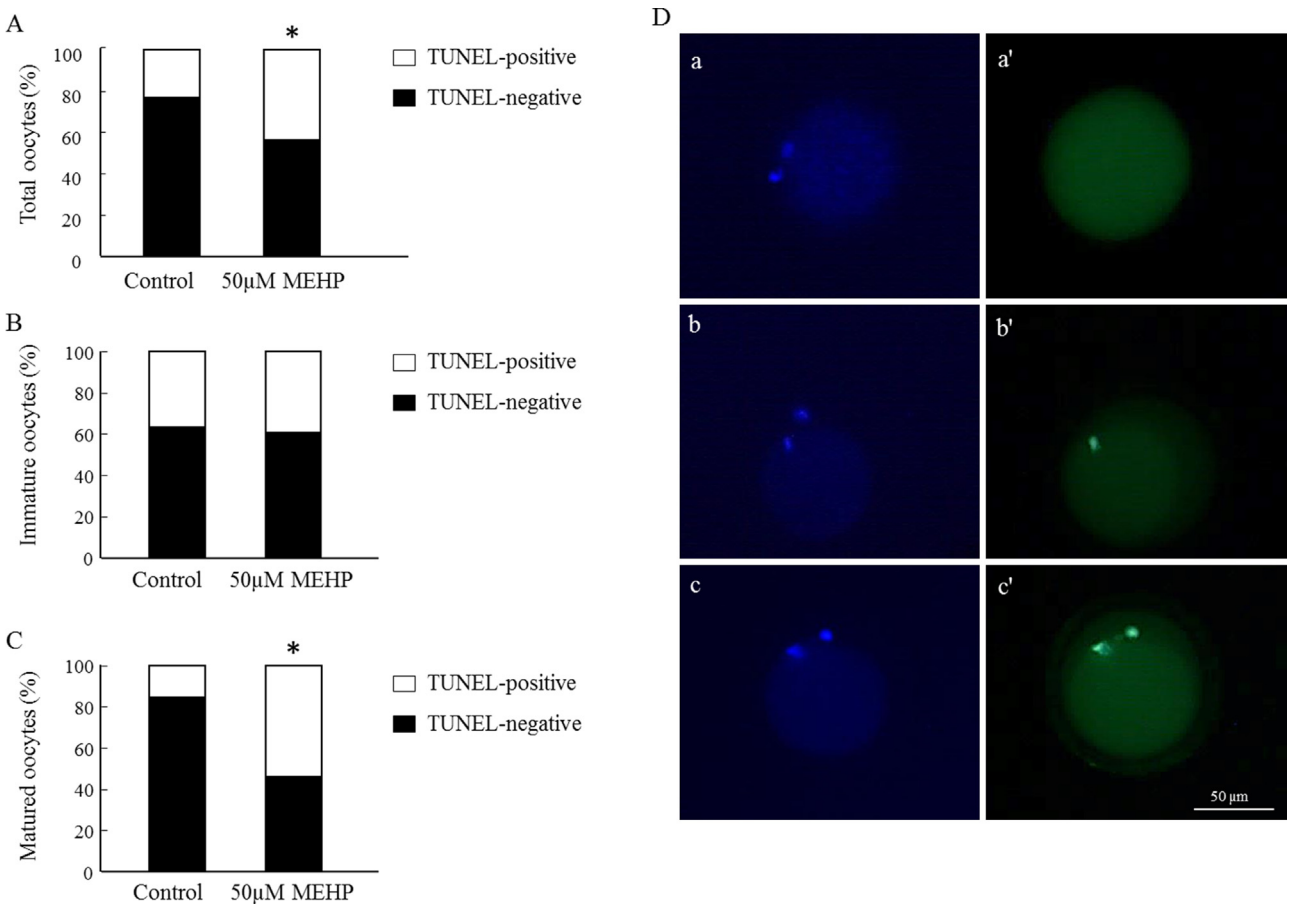

Fig. 2. Effect of MEHP on DNA fragmentation. Oocytes were cultured in OMM without (control) or with 50 μM MEHP, stained with DAPI and subjected to TUNEL assay to evaluate DNA fragmentation. (A) Proportions of TUNEL-positive and TUNEL-negative oocytes out of total number of oocytes in the control and MEHP-treated groups; (B) proportions of TUNEL-positive and TUNEL-negative immature oocytes out of total immature oocytes; (C) proportions of TUNEL-positive and TUNEL-negative mature oocytes out of total mature oocytes; (D) representative images of mature oocytes (a–c) classified with a TUNEL-negative (a′) or TUNEL-positive metaphase plate (b′), or TUNEL-positive labeling of both metaphase plate and polar body (c′). Data are presented as the proportion of TUNEL-positive and TUNEL-negative oocytes calculated out of total (A), immature (B) or mature (C) oocytes. *$P < 0.05$.

mitochondrial category I was numerically higher in the mature vs immature groups (Fig. 3A, D; 41.94% vs. 58.82%) but this difference was not significant ($P < 0.13$).

3.2.3. Cytoplasmic characteristics in immature oocytes

In immature oocytes, the mitochondrial distribution did not differ between control and MEHP-treated groups (Fig. 3A; $P = 0.64$), as reflected by a similar proportion of oocytes in each of the three mitochondrial distribution categories. Similarly, the pattern of CG distribution into the three CG types did not differ between control and MEHP-treated oocytes (Fig. 3B; $P = 0.41$). However, the distribution pattern of oocytes into the three ER classes differed between control and MEHP-treated immature oocytes (Fig. 3C; $P < 0.0003$), characterized by a lower proportion of ER class I oocytes and higher proportion of ER class II oocytes in the MEHP-treated vs. control group (Fig. 3C; 16.67% vs. 40.0%; $P < 0.04$ and 74.32% vs. 44.83%; $P < 0.006$).

3.2.4. Cytoplasmic characteristics in mature oocytes

The reorganization pattern of mitochondria, CGs and ER in mature oocytes was impaired by MEHP ($P < 0.001$), as reflected by a lower proportion of oocytes with mitochondrial category I in MEHP-treated vs. control groups (Figs. 3D and 4A; 58.82% vs. 87.69%; $P < 0.001$). On the other hand, the proportions of mitochondrial categories II and III oocytes were higher in MEHP-treated vs. control groups (Figs. 3D and 4B, C; $P < 0.03$).

MEHP altered CG relocation in mature oocytes, as reflected by a different distribution of oocytes into the CG types (Figs. 3E and 4D–F; $P < 0.01$). In particular, the proportion of type III CG oocytes was lower (Fig. 4D; 37.04% vs. 53.41%; $P < 0.05$), whereas the proportion of type I CG oocytes was higher (Fig. 4F; 38.89% vs. 17.05%; $P < 0.005$) in the MEHP-treated vs. control group.

MEHP impaired ER reorganization in the mature oocytes, as reflected by a decreased proportion of class I ER and an

Table 2
Effects of MEHP on nuclear maturation of bovine COCs.

Group	*N*	Meiotic stages (%)					
		GV	GVBD	MI	AI	TI	MII
Control	321	1.5 ± 0.1[a]	1.8 ± 0.1[a]	4.3 ± 0.1	9.0 ± 0.1	11.8 ± 0.2[a]	69.7 ± 0.4[a]
50 μM MEHP	335	4.1 ± 0.3[b]	4.4 ± 0.1[b]	4.4 ± 0.1	8.9 ± 0.5	22.3 ± 0.4[b]	36.4 ± 0.6[b]

Different superscript letters (a and b) within a column indicate significant difference ($P < 0.05$). Data are presented as mean ± SEM.

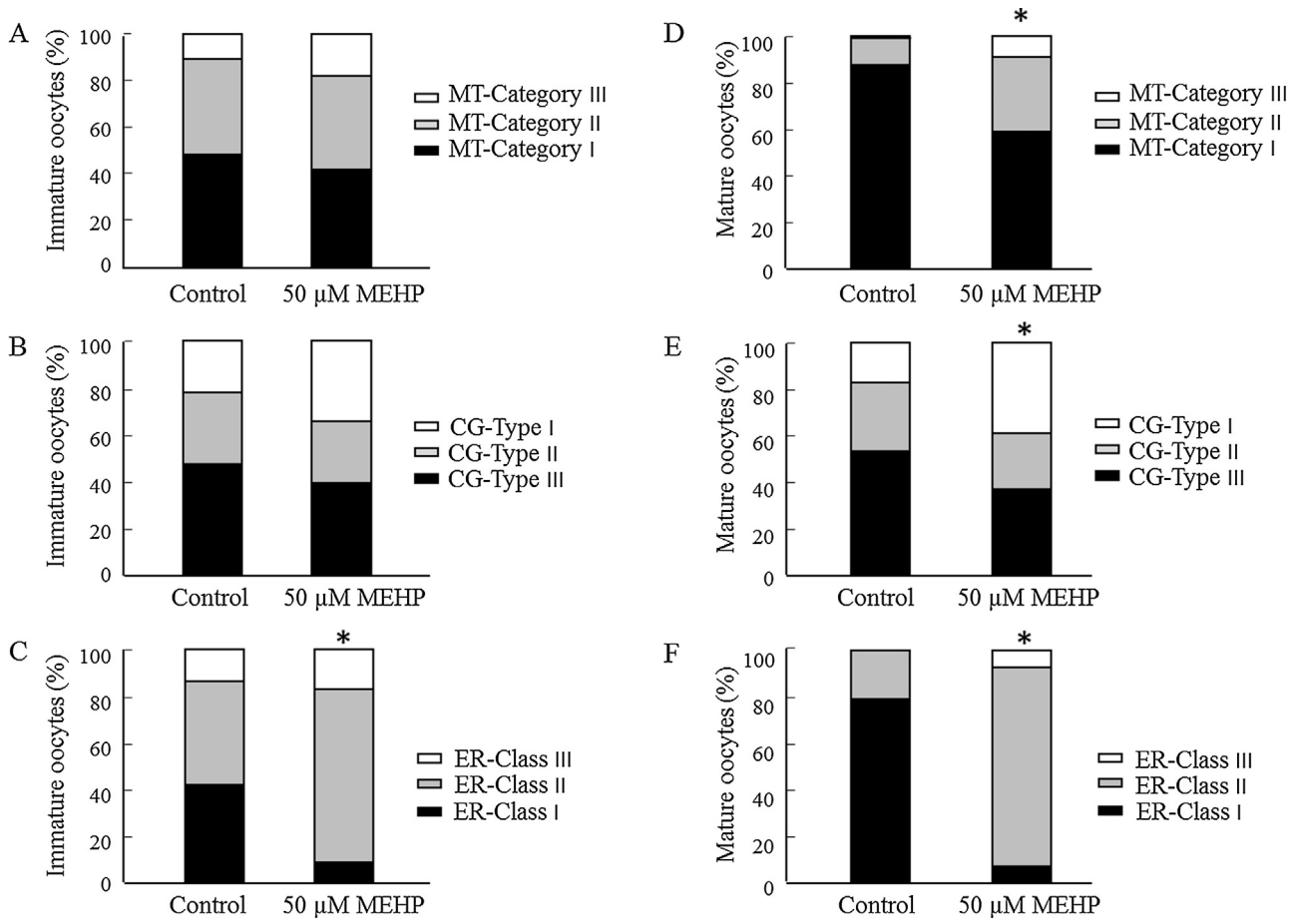

Fig. 3. Cytoplasmic organelle reorganization in oocytes cultured for 22 h in OMM without (control) or with 50 μM MEHP and classified into immature (A–C) and mature (D–F) groups. (A and D) distribution of oocytes into the different mitochondrial (MT) categories (I–III); (B and E) distribution of oocytes into the different CG types (I–III); (C and F) distribution of oocytes into the different ER classes (I–III). Presented is the proportion of oocytes in each category/type/class, calculated out of immature or mature oocytes for each experimental group. *$P < 0.05$.

increased proportion of class II ER oocytes relative to the controls (Figs. 3F and G–I; $P < 0.0001$).

4. Discussion

Phthalates, especially MEHP, have a long-lasting negative effect on oocyte developmental competence: exposing oocytes to MEHP during maturation decreased both cleavage and blastocyst-formation rate [19]. This was associated with negative effects of MEHP on meiotic progression, manifested by a higher proportion of oocytes that did not progress to the MII stage and complete meiosis. Here we provide first evidences that MEHP not only affects meiotic progress but also induces changes in CG migration and ER reorganization, and impairs mitochondrial reorganization and function during oocyte maturation. Moreover, a comparison of mature and immature oocytes revealed that these alterations are more prominently expressed at the MII stage.

In our previous study [19] and in the current study, MEHP-induced negative effects on nuclear maturation. This is also been reported by others: a decreased proportion of MII-stage oocytes was recorded when bovine COCs were exposed to 10, 25, 50, 75 or 100 μM MEHP; no meiotic progression was found at all after denuded oocyte exposure to 50, 75 or 100 μM MEHP for 24 h [27]. A similar negative impact on meiotic progression was found for denuded mouse oocytes that were cultured in vitro with 100, 200 and 400 μM MEHP [55], and for bovine COCs cultured with doses higher than 75 μM MEHP [26]. However, a higher proportion of TI-stage oocytes was found in the MEHP-treated group, suggesting a delay in meiotic progress [18] and [27]. Nevertheless, nuclear maturation by itself is not sufficient to predict embryonic developmental capacity [28,56,57], as oocyte maturation also involves multiple cytoplasmic events that are required for further developmental stages. Relocalization of CGs is commonly used to define cytoplasmic maturation [58,59], and is suggested to underlie the mechanism that eliminates polyspermy [60,61]. It is characterized by conversion of the CG-distribution cluster at the GV stage into a thin layer lining the oolemma at MII. This pattern has been recorded in bovine [40,41], mouse [62], human [63] and porcine [64,65].

In the current study, only a modest correlation between nuclear maturation and CG reorganization was found, with 53.41% of the MII-stage oocytes being defined as CG type III oocytes (i.e., cytoplasmically mature CGs). MEHP interfered with this correlation, as reflected by a 16.4% reduction in the proportion of CG type III oocytes. CG translocation to the oocyte cortex region is required for CG exocytosis, an important mechanism in blocking the abnormal phenomenon of polyspermy in mammals [61]. Aroclor 1254, a mixture of polychlorinated biphenyl (PCB) congeners, known as reproductive toxicants, inhibited CG redistribution in bovine oocytes [66] and slowed the rate of spontaneous CG exocytosis in mice [67]. CG exocytosis is a Ca^{2+}-dependent signaling mechanism [40] and [68] that plays an important role in maturation and embryonic development [69]. It is therefore reasonable to assume that the

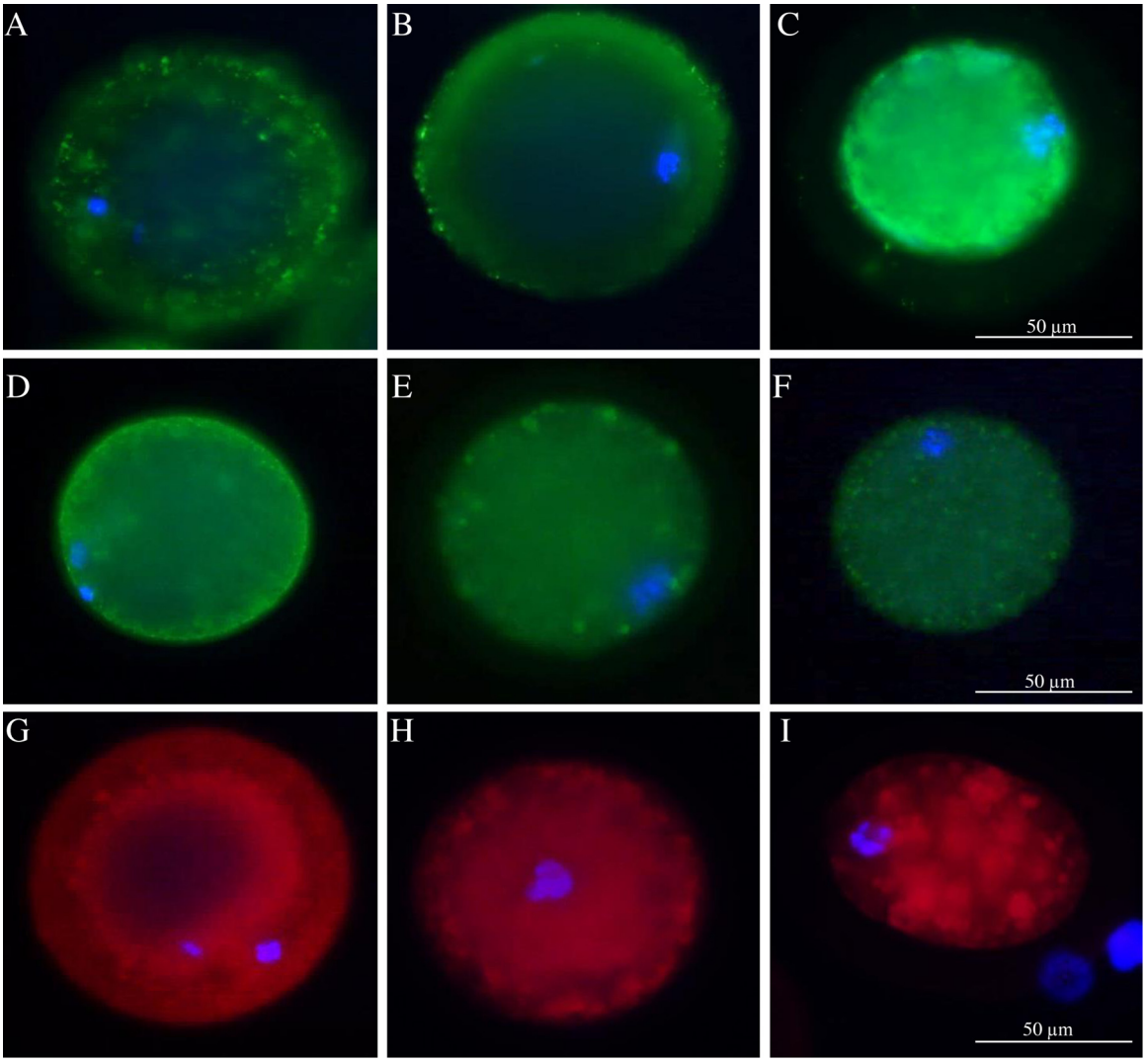

Fig. 4. Representative images of mitochondrial, CG and ER distribution patterns in oocytes. Oocytes were stained with Mitotracker green and counterstained with Hoechst 33342; (A–C) mitochondrial categories I, II and III – mature, immature and degenerated, respectively. Oocytes were stained with FITC-PNA and counterstained with DAPI; (D–F) CG types III, II and I – mature, partially mature and immature, respectively. Oocytes were stained with ER-ID red dye and counterstained with Hoechst 33324; (G–I) ER classes I, II and III – mature, immature and degenerated, respectively. (A, D and G) Representative images of nuclear and cytoplasmically mature oocytes.

MEHP-induced alterations in CG distribution noted in the current study might also involve impairments in the ER, the major site of intracellular calcium storage.

During oocyte maturation, the ER undergoes biochemical and structural changes for proper calcium regulation [70,71]. This has been documented in both humans [38] and mice [37] and [70], expressed by a change in distribution from dispersion throughout the entire cytoplasm at the GV stage to distinct clusters (1–2 μm in diameter) in the cortical region at the MII stage. Analyzing the association between nuclear and cytoplasmic events, we revealed that meiotic progression is highly correlated with ER reorganization since 85.42% of the MII-stage oocytes were classified as ER class I oocytes (i.e., cytoplasmically mature ER). MEHP dramatically increased the proportion of ER class II (i.e., cytoplasmically immature) oocytes and markedly reduced the proportion of ER class I oocytes. A high correlation between the proportion of ER class II oocytes and nuclear stage was found for both immature and mature oocytes in the MEHP group, suggesting that the ER redistribution mechanism is more sensitive to MEHP. Irregular ER redistribution is suggested to interfere with normal temporal Ca^{2+} oscillation, a hallmark of mammalian fertilization needed for egg activation [72], resumption of meiosis and meiotic progression [73]. It has been recently reported that exposure to MEHP increases intracellular Ca^{2+} in rat hepatocytes. With that respect, increased intracellular Ca^{2+} has been suggested as a phthalate-induced mediator of apoptosis [74].

Proper oocyte mitochondrial function is crucial for further embryonic development [75–77]. Therefore, mitochondrial distribution is associated with ATP production and developmental competence [34]. During maturation, the mitochondria shift from a peripheral distribution to dispersion throughout the cytoplasm [33,34]. Stojkovic et al. [34] found that 80% of mitochondrial category I oocytes exhibit first PB extrusion. Here we report classification of 88% of the MII-stage oocytes in the control group as mitochondrial category I; MEHP reduced this proportion to 59%. In support of this, exposure to Aroclor 1254 during porcine maturation altered mitochondrial relocation [78]. Moreover, studies in other cell lines have found the mitochondria to be a main target site for phthalates [79–81]. On the other hand, Ambruosi et al. [18] reported that DEHP does not affect mitochondrial distribution in equine MII-stage oocytes. Differences between studies are most likely due to the chemicals' diverse activities.

The findings of the current study indicated that MEHP not only impaired mitochondria distribution but also CG and ER

relocalization, all of which depend on cytoskeleton-element arrangement [31,82]. Therefore, it is reasonable to assume that MEHP-induced disruption of organelle reorganization involves alterations in the cytoskeleton. This assumption is supported by previous studies in which phthalates were reported to act on the actin cytoskeleton in Py1a rat osteoblasts [83], and DEHP (12.5, 25 and 50 μM) altered the expression of cytoskeleton-related genes in Syrian hamster embryo cells, in particular, upregulating genes involved in actin regulation [84].

In addition, the current study provides new evidence showing that the negative effect of MEHP is not limited to mitochondrial reorganization; it also induces alterations in mitochondrial function, such as membrane polarity and the abundance of transcripts associated with the electron-transport chain. During oocyte maturation, mitochondrial membrane potential increases [85] due to the intensive increase in oxidative metabolism [86]; it is therefore considered an indicator of oocyte developmental competence [51,79,87]. In both humans and mice, insufficient elevation of mitochondrial membrane potential is associated with a high incidence of oocytes that cannot be penetrated by sperm [85], as well as reduced embryonic development [79]. Therefore, the MEHP-induced reduction in mitochondrial polarization reported here might explain the reduced developmental competence upon exposure to MEHP [19]. In support of this, exposure to 50 or 100 μM MEHP for 24 h reduced mitochondrial membrane potential in normal (L02) and hepatomatous (HepG2) human liver cell lines [88]. A similar effect was reported for human TK6 lymphoblasts after treatment with either DEHP or MEHP, occurring in a dose-dependent manner [89].

Moreover, changes in mitochondrial polarity are associated with an increase in ROS. Here we report prominent ROS expression in MEHP-treated oocytes. Accordingly, MEHP has been found to induce oxidative stress via elevation in ROS production in 2-cell-stage mouse embryos [90], mouse antral follicles [91], a human placental cell line [22], rat germ cells [92] and mouse Leydig cells [93]. Chu et al. [90] found that mono-n-butyl phthalate (a metabolite of dibutyl phthalate) increases ROS level and deleteriously affects the developmental progression of mouse embryos. Taken together, it is suggested that MEHP induces changes in mitochondrial membrane potential and increases ROS generation, which in turn cause the mitochondrial dysfunction. Nevertheless, it is not clear whether elevation in ROS production is a result of depolarization of the mitochondrial membrane [94] or by itself causes mitochondrial dysfunction [95,96]. Ghosh et al. [74] suggested that DEHP exposure in rat hepatocytes induces ROS production along with activation of NF-κB and loss of membrane potential.

The MEHP-induced changes in mitochondrial polarity and ROS levels might underlie the increased proportion of oocytes with fragmented DNA, as determined by an increased proportion of TUNEL-positive oocytes out of all mature oocytes (current study). In agreement, we previously documented MEHP-altered expression of the apoptosis-related gene *ASAH1* in mature oocytes and 2-cell-stage embryos [19]. A similar effect on the apoptosis-associated genes *Bcl2* and *Bax* was reported by [91] for mouse antral follicles. Phthalates have also been shown to increase DNA fragmentation in equine cumulus cells [18] and to induce apoptosis in various cell lines [97–99]. Nevertheless, further examination is needed to clarify whether phthalate induces DNA fragmentation via apoptosis, necrosis or other cell-death pathways.

The mitochondrial OXPHOS is unique in that it involves multiple enzymatic complexes and is composed of subunits encoded by both nuclear and mitochondrial genomes [100]. Successful OXPHOS functioning requires a tight interaction within and among enzymatic complexes I–V. Thus, any mismatch in nuclear or mitochondrial gene expression, or both, might impair electron-transport-chain activity and thus ROS generation [101]. Here we provide evidence for MEHP-induced alterations in the expression of both nuclear (*CYC1*, *ATP5B*) and mitochondrial (*MT-CO1*) genes. *CYC1* encodes a subunit of the cytochrome bc1 complex, the third complex in the electron-transport chain. *MT-CO1* encodes one of the three subunits forming the catalytic core of cytochrome c oxidase, the last complex of the electron-transport chain [102]. During maturation, there is an intensive decline in poly(A) RNA caused by both degradation and deadenylation processes [103]. It can therefore be speculated that MEHP interferes with these processes. In support of this assumption, Pocar et al. [66] found that IVM of bovine oocytes in the presence of PCB affects the degree of polyadenylation of specific genes. Nevertheless, as far as we know, these effects have not been reported for phthalates.

While not clear, in the current study, the transcript level of *ATP5B* in the MEHP-treated oocytes was higher than in the controls. *ATP5B* encodes a subunit of F1 – part of ATP synthase (complex V), the soluble catalytic core [104]. During maturation, following GVBD, transcription in the oocyte ceases abruptly [105], thus the increased level of *ATP5B* transcript reported here could be explained by alteration of the poly(A) tail's length due to phthalate's effect on the polyadenylation mechanism. Regardless, the functioning of the OXPHOS system is dependent on each of these complexes therefore, MEHP-induced alterations in one or more of them can impair overall mitochondrial activity, which in turn might lead to insufficient ATP production, known to be critical for oocyte maturation, fertilization, and subsequent embryo development [106].

In summary, results of this study explored the potential risk of exposing bovine oocytes to a relatively high dose (50 μM) of MEHP and its deleterious effects on the oocyte's competence to undergo nuclear and cytoplasmic maturation.

Funding

The study was conducted in the framework of The Hebrew University Center of Excellence in Agriculture and Environmental Health funded by the Environment and Health Fund, Jerusalem, Israel and by the Israeli Ministry of Agriculture (project #821-130-10).

Conflict of interest

The authors declare that there is no conflict of interest that could be perceived as prejudicing the impartiality of the research reported.

Transparency document

The Transparency document associated with this article can be found in the online version.

References

[1] Kavlock R, Barr D, Boekelheide K, Breslin W, Breysse P, Chapin R, et al. NTP-CERHR Expert Panel update on the reproductive and developmental toxicity of di(2-ethylhexyl) phthalate. Reprod Toxicol 2006;22:291–399.
[2] Heudorf U, Mersch-Sundermann V, Angerer J. Phthalates: toxicology and exposure. Int J Hyg Environ Health 2007;210:623–34.
[3] Balabanič D, Rupnik M, Klemenčič AK. Negative impact of endocrine-disrupting compounds on human reproductive health. Reprod Fertil Dev 2011;23:403–16.
[4] Johnson KJ, Heger NE, Boekelheide K. Of mice and men (and rats): phthalate-induced fetal testis endocrine disruption is species-dependent. Toxicol Sci 2012;129:235–48.
[5] Kay VR, Chambers C, Foster WG. Reproductive and developmental effects of phthalate diesters in females. Crit Rev Toxicol 2013;43:200–19.
[6] EFSA Scientific Committee. Scientific opinion on the hazard assessment of endocrine disruptors: scientific criteria for identification of endocrine disruptors and appropriateness of existing test methods for assessing effects mediated by these substances on human health and the environment. EFSA J 2013;11:3132.

[7] Calafat AM, Needham LL, Silva MJ, Lambert G. Exposure to di-(2-ethylhexyl) phthalate among premature neonates in a neonatal intensive care unit. Pediatrics 2004;113:e429–34.
[8] Inoue K, Kawaguchi M, Yamanaka R, Higuchi T, Ito R, Saito K, et al. Evaluation and analysis of exposure levels of di(2-ehylhexyl) phthalate from blood bags. Clin Chim Acta 2005;358:159–66.
[9] Rael LT, Bar-Or R, Ambruso DR, Mains CW, Slone DS, Craun ML, et al. Phthalate esters used as plasticizers in packed red blood cell storage bags may lead to progressive toxin exposure and the release of pro-inflammatory cytokines. Oxid Med Cell Longev 2009;2:166–71.
[10] Frederiksen H, Jørgensen N, Andersson AM. Correlations between phthalate metabolites in urine, serum, and seminal plasma from young Danish men determined by isotope dilution liquid chromatography tandem mass spectrometry. J Anal Toxicol 2010;34:400–10.
[11] Latini G, De Felice C, Presta G, Del Vecchio A, Paris I, Ruggieri F, et al. In utero exposure to di-(2-ethylhexyl) phthalate and duration of human pregnancy. Environ Health Perspect 2003;111:1783–5.
[12] Hoppin JA, Brock JW, Davis BJ, Baird DD. Reproducibility of urinary phthalate metabolites in first morning urine samples. Environ Health Perspect 2002;110:515–8.
[13] Duty SM, Ackerman RM, Calafat AM, Hauser R. Personal care product use predicts urinary concentrations of some phthalate monoesters. Environ Health Perspect 2005;113:1530–5.
[14] Cobellis L, Latini G, De Felice C, Razzi S, Paris I, Ruggieri F, et al. High plasma concentration of di-(2-ethylhexyl)-phthalate in women with endometriosis. Hum Reprod 2003;18:1512–5.
[15] Silva MJ, Reidy JA, Herbert AR, Preau Jr JL, Needham LL, Calafat AM. Detection of phthalate metabolites in human amniotic fluid. Bull Environ Contam Toxicol 2004;72:1226–31.
[16] Zhang T, Li L, Qin XS, Zhou Y, Zhang XF, Wang LQ, et al. Di-(2-ethylhexyl) phthalate and bisphenol A exposure impairs mouse primordial follicle assembly *in vitro*. Environ Mol Mutagen 2014;55:343–53.
[17] Gupta RK, Singh JM, Leslie TC, Meachum S, Flaws JA, Yao HH. Di-(2-ethylhexyl) phthalate and mono-(2-ethylhexyl) phthalate inhibit growth and reduce estradiol levels of antral follicles *in vitro*. Toxicol Appl Pharmacol 2010;242:224–30.
[18] Ambruosi B, Uranio MF, Sardanelli AM, Pocar P, Martino NA, Paternoster MS, et al. In vitro acute exposure to DEHP affects oocyte meiotic maturation, energy and oxidative stress parameters in a large animal model. PLoS ONE 2011;6:e27452.
[19] Grossman D, Kalo D, Gendelman M, Roth Z. Effect of di-(2-ethylhexyl) phthalate and mono-(2-ethylhexyl) phthalate on in vitro developmental competence of bovine oocytes. Cell Biol Toxicol 2012;28:383–96.
[20] Huang XF, Li Y, Gu YH, Liu M, Xu Y, Yuan Y, et al. The effects of di-(2-ethylhexyl)-phthalate exposure on fertilization and embryonic development in vitro and testicular genomic mutation in vivo. PLoS ONE 2012;7:e50465.
[21] Lenie S, Smitz J. Steroidogenesis-disrupting compounds can be effectively studied for major fertility-related endpoints using in vitro cultured mouse follicles. Toxicol Lett 2009;185:143–52.
[22] Tetz LM, Cheng AA, Korte CS, Giese RW, Wang P, Harris C, et al. Mono-2-ethylhexyl phthalate induces oxidative stress responses in human placental cells in vitro. Toxicol Appl Pharmacol 2013;268:47–54.
[23] Wan X, Zhu Y, Ma X, Zhu J, Zheng Y, Hou J, et al. Effect of DEHP and its metabolite MEHP on in vitro rat follicular development. Wei Sheng Yan Jiu 2010;39, 268–270, 274.
[24] Bonilla E, del Mazo J. Deregulation of the Sod1 and Nd1 genes in mouse fetal oocytes exposed to mono-(2-ethylhexyl) phthalate (MEHP). Reprod Toxicol 2010;30:387–92.
[25] Smith GD. In vitro maturation of oocytes. Curr Womens Health Rep 2001;1:143–51.
[26] Beker van Woudenberg A, Gröllers-Mulderij M, Snel C, Jeurissen N, Stierum R, Wolterbeek A. The bovine oocyte in vitro maturation model: a potential tool for reproductive toxicology screening. Reprod Toxicol 2012;34:251–60.
[27] Anas MK, Suzuki C, Yoshioka K, Iwamura S. Effect of mono-(2-ethylhexyl) phthalate on bovine oocyte maturation in vitro. Reprod Toxicol 2003;17:305–10.
[28] Eppig JJ. Coordination of nuclear and cytoplasmic oocyte maturation in eutherian mammals. Reprod Fertil Dev 1996;8:485–9.
[29] Brevini-Gandolfi TAL, Gandolfi F. The maternal legacy to the embryo: cytoplasmic components and their effects on early development. Theriogenology 2001;55:1255–76.
[30] Watson AJ. Oocyte cytoplasmic maturation: a key mediator of oocyte and embryo developmental competence. J Anim Sci 2007;85:E1–3.
[31] Ferreira EM, Vireque AA, Adona PR, Meirelles FV, Ferriani RA, Navarro PAAS. Cytoplasmic maturation of bovine oocytes: structural and biochemical modifications and acquisition of developmental competence. Theriogenology 2009;71:836–48.
[32] Yamada M, Isaji Y. Structural and functional changes linked to, and factors promoting, cytoplasmic maturation in mammalian oocytes. Reprod Med Biol 2011;10:69–79.
[33] Kruip TAM, Cran DG, van Beneden TH, Dieleman SJ. Structural changes in bovine oocytes during final maturation in vivo. Gamete Res 1983;8:29–47.
[34] Stojkovic M, Machado SA, Stojkovic P, Zakhartchenko V, Hutzler P, Gonçalves PB, et al. Mitochondrial distribution and adenosine triphosphate content of bovine oocytes before and after in vitro maturation: correlation with morphological criteria and developmental capacity after in vitro fertilization and culture. Biol Reprod 2001;64:904–9.
[35] Mehlmann LM, Terasaki M, Jaffe LA, Kline D. Reorganization of the endoplasmic reticulum during meiotic maturation of the mouse oocyte. Dev Biol 1995;170:607–15.
[36] Shiraishi K, Okada A, Shirakawa H, Nakanishi S, Mikoshiba K, Miyazaki S. Developmental changes in the distribution of the endoplasmic reticulum and inositol 1,4,5-trisphosphate receptors and the spatial pattern of Ca^{2+} release during maturation of hamster oocytes. Dev Biol 1995;170:594–606.
[37] FitzHarris G, Marangos P, Carroll J. Changes in endoplasmic reticulum structure during mouse oocyte maturation are controlled by the cytoskeleton and cytoplasmic dynein. Dev Biol 2007;305:133–44.
[38] Mann JS, Lowther KM, Mehlmann LM. Reorganization of the endoplasmic reticulum and development of Ca^{2+} release mechanisms during meiotic maturation of human oocytes. Biol Reprod 2010;83:578–83.
[39] Payne C, Schatten G. Golgi dynamics during meiosis are distinct from mitosis and are coupled to endoplasmic reticulum dynamics until fertilization. Dev Biol 2003;264:50–63.
[40] Hosoe M, Shioya Y. Distribution of cortical granules in bovine oocytes classified by cumulus complex. Zygote 1997;5:371–6.
[41] Izadyar F, Hage WJ, Colenbrander B, Bevers MM. The promotory effect of growth hormone on the developmental competence of in vitro matured bovine oocytes is due to improved cytoplasmic maturation. Mol Reprod Dev 1998;49:444–53.
[42] Ducibella T, Duffy P, Buetow J. Quantification and localization of cortical granules during oogenesis in the mouse. Biol Reprod 1994;50:467–73.
[43] Eppig JJ, Schultz RM, O'Brien M, Chesnel F. Relationship between the developmental programs controlling nuclear and cytoplasmic maturation of mouse oocytes. Dev Biol 1994;164:1–9.
[44] Gendelman M, Aroyo A, Yavin S, Roth Z. Seasonal effects on gene expression, cleavage timing, and developmental competence of bovine preimplantation embryos. Reproduction 2010;140:73–82.
[45] Koyama K, Kang SS, Huang W, Yanagawa Y, Takahashi Y, Nagano M. Aging-related changes in in vitro-matured bovine oocytes: oxidative stress, mitochondrial activity and ATP content after nuclear maturation. J Reprod Dev 2014;60:136–42.
[46] Park SH, Cho HS, Yu IJ. Effect of bovine follicular fluid on reactive oxygen species and glutathione in oocytes, apoptosis and apoptosis-related gene expression of in vitro-produced blastocysts. Reprod Domest Anim 2014;49:370–7.
[47] Wang F, Tian X, Zhang L, He C, Ji P, Li Y, et al. Beneficial effect of resveratrol on bovine oocyte maturation and subsequent embryonic development after in vitro fertilization. Fertil Steril 2014;101:577–86.
[48] Gendelman M, Roth Z. Incorporation of coenzyme Q10 into bovine oocytes improves mitochondrial features and alleviates the effects of summer thermal stress on developmental competence. Biol Reprod 2012;87:118.
[49] Kalo D, Roth Z. Involvement of the sphingolipid ceramide in heat-shock-induced apoptosis of bovine oocytes. Reprod Fertil Dev 2011;23:876–88.
[50] Sun QY, Wu GM, Lai L, Park KW, Cabot R, Cheong HT, et al. Translocation of active mitochondria during pig oocyte maturation, fertilization and early embryo development in vitro. Reproduction 2001;122:155–63.
[51] Wilding M, Dale B, Marino M, di Matteo L, Alviggi C, Pisaturo ML, et al. Mitochondrial aggregation patterns and activity in human oocytes and preimplantation embryos. Hum Reprod 2001;16:909–17.
[52] Brevini TA, Vassena R, Francisci C, Gandolfi F. Role of adenosine triphosphate, active mitochondria, and microtubules in the acquisition of developmental competence of parthenogenetically activated pig oocytes. Biol Reprod 2005;72:1218–23.
[53] Dalton CM, Carroll J. Biased inheritance of mitochondria during asymmetric cell division in the mouse oocyte. J Cell Sci 2013;126:2955–64.
[54] Asaf S, Leitner G, Furman O, Lavon Y, Kalo D, Wolfenson D, et al. Effectsof *Escherichia coli*- and *Staphylococcus aureus*-induced mastitis in lactating cows on oocyte developmental competence. Reproduction 2013;147:33–43.
[55] Dalman A, Eimani H, Sepehri H, Ashtiani SK, Valojerdi MR, Eftekhari-Yazdi P, et al. Effect of mono-(2-ethylhexyl) phthalate (MEHP) on resumption of meiosis, in vitro maturation and embryo development of immature mouse oocytes. Biofactors 2008;33:149–55.
[56] Thibault CG. Final stages of mammalian oocyte maturation. In: Biggers JD, Schuetz AW, editors. Oogenesis. Baltimore, MD: University Park Press; 1972. p. 397–411.
[57] Fulka Jr J, First NL, Moor RM. Nuclear and cytoplasmic determinants involved in the regulation of mammalian oocyte maturation. Mol Hum Reprod 1998;4:41–9.
[58] Damiani P, Fissore RA, Cibelli JB, Long CR, Balise JJ, Robl JM, et al. Evaluation of developmental competence, nuclear and ooplasmic maturation of calf oocytes. Mol Reprod Dev 1996;45:521–34.
[59] Miyara F, Aubriot FX, Glissant A, Nathan C, Douard S, Stanovici A, et al. Multiparameter analysis of human oocytes at metaphase II stage after IVF failure in non-male infertility. Hum Reprod 2003;18:1494–503.
[60] Ducibella T. The cortical reaction and development of activation competence in mammalian oocytes. Hum Reprod Update 1996;2:29–42.
[61] Liu M. The biology and dynamics of mammalian cortical granules. Reprod Biol Endocrinol 2011;9:149.
[62] Liu XY, Mal SF, Miao DQ, Liu DJ, Bao S, Tan JH. Cortical granules behave differently in mouse oocytes matured under different conditions. Hum Reprod 2005;20:3402–13.

[63] Liu S, Li Y, Feng HL, Yan JH, Li M, Ma SY, et al. Dynamic modulation of cytoskeleton during in vitro maturation in human oocytes. Am J Obstet Gynecol 2010;203, 151.e1–151.e7.
[64] Kim NH, Day BN, Lee HT, Chung KS. Microfilament assembly and cortical granule distribution during maturation, parthenogenetic activation and fertilisation in the porcine oocyte. Zygote 1996;4:145–9.
[65] Wang WH, Hosoe M, Shioya Y. Induction of cortical granule exocytosis of pig oocytes by spermatozoa during meiotic maturation. J Reprod Fertil 1997;109:247–55.
[66] Pocar P, Brevini TA, Perazzoli F, Cillo F, Modina S, Gandolfi F. Cellular and molecular mechanisms mediating the effects of polychlorinated biphenyls on oocyte developmental competence in cattle. Mol Reprod Dev 2001;60:535–41.
[67] Greenfeld CR, Xiongqing W, Dukelow WR. Aroclor 1254 does not affect the IVF of cumulus-free mouse oocytes. Bull Environ Contam Toxicol 1998;60:766–72.
[68] Abbott AL, Ducibella T. Calcium and the control of mammalian cortical granule exocytosis. Front Biosci 2001;6:D792–806.
[69] Machaca K. Ca^{2+} signaling differentiation during oocyte maturation. J Cell Physiol 2007;213:331–40.
[70] Kline D. Attributes and dynamics of the endoplasmic reticulum in mammalian eggs. Curr Top Dev Biol 2000;50:125–54.
[71] Ajduk A, Małagocki A, Maleszewski M. Cytoplasmic maturation of mammalian oocytes: development of a mechanism responsible for sperm-induced Ca^{2+} oscillations. Reprod Biol 2008;8:3–22.
[72] Ducibella T, Huneau D, Angelichio E, Xu Z, Schultz RM, Kopf GS, et al. Egg-to-embryo transition is driven by differential responses to Ca(2+) oscillation number. Dev Biol 2002;250:280–91.
[73] Homa ST. Calcium and meiotic maturation of the mammalian oocyte. Mol Reprod Dev 1995;40:122–34.
[74] Ghosh J, Das J, Manna P, Sil PC. Hepatotoxicity of di-(2-ethylhexyl)phthalate is attributed to calcium aggravation, ROS-mediated mitochondrial depolarization, and ERK/NF-κB pathway activation. Free Radic Biol Med 2010;49:1779–91.
[75] Bavister BD, Squirrell JM. Mitochondrial distribution and function in oocytes and early embryos. Hum Reprod 2000;15:189–98.
[76] Acton BM, Jurisicova A, Jurisica I, Casper RF. Alterations in mitochondrial membrane potential during preimplantation stages of mouse and human embryo development. Mol Hum Reprod 2004;10:23–32.
[77] Thouas GA, Trounson AO, Wolvetang EJ, Jones GM. Mitochondrial dysfunction in mouse oocytes results in preimplantation embryo arrest in vitro. Biol Reprod 2004;71:1936–42.
[78] Brevini TA, Vassena R, Paffoni A, Francisci C, Fascio U, Gandolfi F. Exposure of pig oocytes to PCBs during in vitro maturation: effects on developmental competence, cytoplasmic remodelling and communications with cumulus cells. Eur J Histochem 2004;48:347–56.
[79] Melnick RL, Schiller CM. Mitochondrial toxicity of phthalate esters. Environ Health Perspect 1982;45:51–6.
[80] Oishi S. Effects of phthalic acid esters on testicular mitochondrial functions in the rat. Arch Toxicol 1990;64:143–7.
[81] Yang G, Zhou X, Wang J, Zhang W, Zheng H, Lu W, et al. MEHP-induced oxidative DNA damage and apoptosis in HepG2 cells correlates with p53-mediated mitochondria-dependent signaling pathway. Food Chem Toxicol 2012;50:2424–31.
[82] Sun QY, Schatten H. Regulation of dynamic events by microfilaments during oocyte maturation and fertilization. Reproduction 2006;131:193–205.
[83] Marchetti L, Sabbieti MG, Menghi M, Materazzi S, Hurley MM, Menghi G. Effects of phthalate esters on actin cytoskeleton of Py1a rat osteoblasts. Histol Histopathol 2002;17:1061–6.
[84] Landkocz Y, Poupin P, Atienzar F, Vasseur P. Transcriptomic effects of di-(2-ethylhexyl)-phthalate in Syrian hamster embryo cells: an important role of early cytoskeleton disturbances in carcinogenesis? BMC Genomics 2011;12:524.
[85] Van Blerkom J, Davis P. Mitochondrial signaling and fertilization. Mol Hum Reprod 2007;13:759–70.
[86] Motta PM, Nottola SA, Makabe S, Heyn R. Mitochondrial morphology in human fetal and adult female germ cells. Hum Reprod 2000;15:129–47.
[87] Van Blerkom J, Davis P, Mathwig V, Alexander S. Domains of high-polarized and low-polarized mitochondria may occur in mouse and human oocytes and early embryos. Hum Reprod 2002;17:393–406.
[88] Chen X, Wang J, Qin Q, Jiang Y, Yang G, Rao K, et al. Mono-2-ethylhexyl phthalate induced loss of mitochondrial membrane potential activation of Caspase3 in HepG2 cells. Environ Toxicol Pharmacol 2012;33:421–30.
[89] Rosado-Berrios CA, Vélez C, Zayas B. Mitochondrial permeability and toxicity of di ethylhexyl and mono ethylhexyl phthalates on TK6 human lymphoblasts cells. Toxicol In Vitro 2011;25:2010–6.
[90] Chu DP, Tian S, Qi L, Hao CJ, Xia HF, Ma X. Abnormality of maternal-to-embryonic transition contributes to MEHP-induced mouse 2-cell block. J Cell Physiol 2013;228:753–63.
[91] Wang W, Craig ZR, Basavarajappa MS, Hafner KS, Flaws JA. Mono-(2-ethylhexyl) phthalate induces oxidative stress and inhibits growth of mouse ovarian antral follicles. Biol Reprod 2012;87:152.
[92] Kasahara E, Sato EF, Miyoshi M, Konaka R, Hiramoto K, Sasaki J, et al. Role of oxidative stress in germ cell apoptosis induced by di(2-ethylhexyl)phthalate. Biochem J 2002;365:849–56.
[93] Erkekoglu P, Rachidi W, Yuzugullu OG, Giray B, Favier A, Ozturk M, et al. Evaluation of cytotoxicity and oxidative DNA damaging effects of di(2-ethylhexyl)-phthalate (DEHP) and mono(2-ethylhexyl)-phthalate (MEHP) on MA-10 Leydig cells and protection by selenium. Toxicol Appl Pharmacol 2010;248:52–62.
[94] Gottlieb E, Vander Heiden MG, Thompson CB. Bcl-x(L) prevents the initial decrease in mitochondrial membrane potential and subsequent reactive oxygen species production during tumor necrosis factor alpha-induced apoptosis. Mol Cell Biol 2000;20:5680–9.
[95] Weiss JN, Korge P, Honda HM, Ping P. Role of the mitochondrial permeability transition in myocardial disease. Circ Res 2003;93:292–301.
[96] Batandier C, Leverve X, Fontaine E. Opening of the mitochondrial permeability transition pore induces reactive oxygen species production at the level of the respiratory chain complex I. J Biol Chem 2004;279:17197–204.
[97] Aung KH, Win-Shwe TT, Kanaya M, Takano H, Tsukahara S. Involvement of hemeoxygenase-1 in di(2-ethylhexyl) phthalate (DEHP)-induced apoptosis of Neuro-2a cells. J Toxicol Sci 2014;39:217–29.
[98] Chu DP, Tian S, Sun DG, Hao CJ, Xia HF, Ma X. Corrigendum to: exposure to mono-n-butyl phthalate disrupts the development of preimplantation embryos. Reprod Fertil Dev 2014;26:491.
[99] Yang G, Zhang W, Qin Q, Wang J, Zheng H, Xiong W, et al. Mono(2-ethylhexyl) phthalate induces apoptosis in p53-silenced L02 cells via activation of both mitochondrial and death receptor pathways. Environ Toxicol 2014, http://dx.doi.org/10.1002/tox.21990.
[100] Thundathil J, Filion F, Smith LC. Molecular control of mitochondrial function in preimplantation mouse embryos. Mol Reprod Dev 2005;71:405–13.
[101] Lane N. Mitonuclear match: optimizing fitness and fertility over generations drives ageing within generations. Bioessays 2011;33:860–9.
[102] Fontanesi F, Soto IC, Barrientos A. Cytochrome c oxidase biogenesis: new levels of regulation. IUBMB Life 2008;60:557–68.
[103] Paynton BV, Rempel R, Bachvarova R. Changes in state of adenylation and time course of degradation of maternal mRNAs during oocyte maturation and early embryonic development in the mouse. Dev Biol 1988;129:304–14.
[104] Wittig I, Schägger H. Structural organization of mitochondrial ATP synthase. Biochim Biophys Acta 2008;1777:592–8.
[105] Tomek W, Torner H, Kanitz W. Comparative analysis of protein synthesis, transcription and cytoplasmic polyadenylation of mRNA during maturation of bovine oocytes in vitro. Reprod Domest Anim 2002;37:86–91.
[106] Van Blerkom J, Davis P, Lee J. ATP content of human oocytes and developmental potential and outcome after *in vitro* fertilization and embryo transfer. Hum Reprod 1995;10:415–24.